Journal of Glaciology

Article

Cite this article: Clemens-Sewall D, Polashenski C, Perovich D, Webster MA (2024). The importance of sub-meter-scale snow roughness on conductive heat flux of Arctic sea ice. *Journal of Glaciology* 1–6. https://doi.org/10.1017/jog.2023.105

Received: 13 May 2023
Revised: 9 December 2023
Accepted: 18 December 2023

Keywords:
Laser altimetry; snow; sea ice; wind-blown snow

Corresponding author:
David Clemens-Sewall;
Email: dcsewall@ucar.edu

cambridge.org/jog

The importance of sub-meter-scale snow roughness on conductive heat flux of Arctic sea ice

David Clemens-Sewall[1,2], Chris Polashenski[1,3], Don Perovich[1] and Melinda Anne Webster[4,5]

[1]Thayer School of Engineering at Dartmouth College, Hanover, NH, USA; [2]NSF National Center for Atmospheric Research, Boulder, CO, USA; [3] Cold Regions Research and Engineering Laboratory, US Army Corps of Engineers, Hanover, NH, USA; [4]Polar Science Center, Applied Physics Laboratory, University of Washington, Seattle, WA, USA and [5]Geophysical Institute, University of Alaska Fairbanks, Fairbanks, AK, USA

Abstract

The conductive heat flux through the snow and ice is a critical component of the mass and energy budgets in the Arctic sea ice system. We use high horizontal resolution (3–15 cm) measurements of snow topography to explore the impacts of sub-meter-scale snow surface roughness on heat flux as simulated by the Finite Element method. Simulating horizontal heat flux in a variable snow cover modestly increases the total simulated heat flux. With horizontal heat flux, as opposed to simple 1D-vertical heat flux modeling, the simulated heat flux is 10% greater than that for uniform snow with the same mean snow thickness for a 31.5 × 21 m region of sea ice (the largest region we studied). Vertical-only (1D) heat flux simulates just a 6% increase for the same region. However, this is highly dependent on observation resolution. Had we measured the snow cover at 1 m horizontal spacing or greater, simulating horizontal heat flux would not have changed the net heat flux from that simulated with vertical-only heat flux. These findings suggest that measuring and modeling snow roughness at sub-meter horizontal scales may be necessary to accurately represent horizontal heat flux on level Arctic sea ice.

1. Motivation and introduction

The decline of Arctic sea ice is a dramatic consequence of and contributor to climate change (e.g., Screen and Simmonds, 2010). However, the observed decline is not fully captured by climate models (Notz and SIMIP Community, 2020). Of the many uncertainties in the sea ice component of climate models, our lack of understanding of how much heat flows through snow and sea ice in winter is one of the greatest uncertainties impacting the amount of Arctic sea ice that models simulate (Urrego-Blanco and others, 2016). The spatial distribution of snow on sea ice is a factor governing this heat flow.

Wind-driven snow redistribution produces a snow cover on Arctic sea ice in which the spatial variability in snow depth is a substantial fraction of the mean, even on level ice. Mallett and others (2022) analyzed 499 snow depth transects (each at least 500 m long) on multi-year ice collected from 1955–1991 and found that the average coefficient of variation, the ratio of the standard deviation to the mean, was 0.417. We tabulated this metric for an additional 24 sites of level, first-year ice (Iacozza and Barber, 1999; Sturm and others, 2002a; Petrich and others, 2012; Webster and others, 2015; Moon and others, 2019) and found an average coefficient of variation of 0.42. Individual sites varied from 0.23 to 0.94. The mean snow depth across these sites was 20.0 cm and the mean standard deviation was 8.5 cm.

Due to fundamental thermodynamics (Fourier, 1822; Sturm and others, 2002b), small-scale (i.e., centimeters to 100 s of meters) spatial variability in snow depth on Arctic sea ice enhances the total amount of conductive heat flux through the snow and ice covers compared to what the conductive heat flux would be for a uniform snow cover with the same mean snow thickness. Conceptually, we can divide this heat flux enhancement into two components based on how we approximate heat flux in models: that which occurs in a 'vertical-only' 1D heat flux simulation and that which is simulated with the full 3D heat fluxes–which we term 'including horizontal' heat flux. Vertical-only simulation is well known and has been implemented in models (e.g., Abraham and others, 2015). In contrast, just two published works (Sturm and others, 2002b; Popović and others, 2020) have explored including horizontal heat flux simulation on Arctic sea ice, with potentially contradictory findings (discussed below). However, to our knowledge there are no published assessments of the relevant spatial resolution for horizontal heat flux simulation. We address this gap through heat flux simulations using 3–15 cm horizontal resolution measurements of snow surface topography.

Snow is ~10 times more thermally insulating than sea ice (Sturm and others, 2002b). The reason horizontal heat flux is potentially important is that it can reduce the net thermal resistivity of the snow-ice system by transporting heat laterally through the relatively conductive ice to areas of thinner snow (at the cost of a longer transport path length in the ice). Consider a thought experiment: you are at the base of a uniform, 1-m-thick sheet of ice with 20 cm of snow directly above you. You have to choose between heat transport pathways that go directly

https://doi.org/10.1017/jog.2023.105 Published online by Cambridge University Press

vertically above you and diagonally through the ice and then through a thinner snow cover. How much thinner does the snow on the diagonal pathway have to be for the diagonal path to be preferable (lower total thermal resistivity) to the vertical pathway? At small horizontal distances, the diagonal distance through the ice is barely greater than the vertical distance. So even small reductions in snow thickness would result in a preferable heat transport pathway. However, as the horizontal distance increases beyond the ice thickness (1 m in this case), the increase in the diagonal distance approaches the increase in the horizontal distance because the cosine of the angle between the diagonal and horizontal approaches one. Thus, much thinner snow, relative to the vertical or shorter diagonal pathways, would be necessary to make longer diagonal pathways preferable. Albeit highly simplified, this thought experiment provides intuition that sub-meter-scale variability in snow depth is likely to be the most important spatial scale of snow depth variability for horizontal heat flux enhancement. Indeed, this thought experiment was the inspiration for the more technical analysis herein.

Anecdotal experience with snow on Arctic sea indicates that there is considerable depth variability on sub-meter length scales, although there is limited published evidence. From semivariograms (Isaaks and Srivastava, 1989) of snow depth (Iacozza and Barber, 1999; Sturm and others, 2002a; Liston and others, 2018), we estimate that the combination of sub-meter-scale snow depth variability and measurement uncertainty has a standard deviation of 2.5–5 cm. Semivariogram analysis of these data cannot distinguish measurement uncertainty from spatial variability at this scale. Combining the potential for sub-meter-scale snow depth variability with the thought experiment above leads to our hypothesis that it may be important to include sub-meter-scale variability and horizontal heat fluxes when simulating the impacts of snow spatial variability on net conductive heat flux for level, Arctic sea ice.

In this work, we focus solely on the impacts of spatial variability of snow depth. Thus, we will consider only steady-state heat conduction with constant values of thermal conductivity in the snow and ice, and no sources or sinks of heat inside the snow-ice system. These simplifications are commonly made (e.g., Abraham and others, 2015; Popović and others, 2020). The impacts of non-conductive heat transport mechanisms such as vapor diffusion (Calonne and others, 2014), convection (Sturm and Johnson, 1991; Colbeck, 1997), and brine drainage (Niedrauer and Martin, 1979) are beyond the scope of this study but may merit further investigation. For brevity, "conductive heat flux" is shortened to "heat flux" throughout this manuscript. With these simplifications, the temperature distribution in the snow and ice is mathematically represented by the solution to Laplace's Equation (Eqn. (1); Laplace, 1822) and the heat flux at any location within the snow and ice is given by Fourier's Law (Eqn. (2); Fourier, 1822):

$$\nabla \cdot \big(\kappa(x, y, z)\nabla T(x, y, z)\big) = 0 \tag{1}$$

$$\vec{q}(x, y, z) = -\kappa(x, y, z)\nabla T(x, y, z) \tag{2}$$

where T is the temperature; κ is the thermal conductivity; and $\vec{q}$ is the heat flux. If the heat flux were only vertical, then the steady state conductive heat flux (which we denote q_v) would simplify to (Eqn. (3): Semtner, 1976):

$$q_v(x, y) = \frac{T_o - T_a}{(h_s(x, y)/\kappa_s) + (h_i(x, y)/\kappa_i)} \tag{3}$$

where T_o and T_a are the temperatures at the ocean-ice and snow-air interfaces respectively; h_s and h_i are the snow depth and ice thickness respectively; and κ_s and κ_i are the snow and ice thermal conductivities respectively. Equation (3) assumes that the snow-air interface temperature is spatially uniform. In theory, spatial variability in conductive heat flux should produce spatial variability in surface temperature that would be balanced by variability in outgoing longwave radiation. However, spatially-resolved measurements of skin temperatures on level ice on the MOSAiC Expedition from a helicopter-borne thermal infrared camera (Thielke and others, 2021) showed minimal spatial variability in skin temperature due to snow depth variability. In this work we will assume the snow-air interface temperature is spatially uniform. Note that if the snow and ice thicknesses were uniform, then all net heat flux would be vertical and uniform.

Vertical-only heat flux simulations are a convenient way to estimate the additional heat flux due to snow spatial variability for two reasons. First, it can be calculated from a collection of independent point measurements of snow and ice thickness (e.g., a transect or stake array). For logistical reasons, most measurements of snow depth and ice thickness come from transects or stake arrays with (sometimes non-uniform) measurements spacing of 1–10 meters (e.g., Hanson, 1965, 1980; Radionov and others, 1997; Sturm and others, 2002a; Perovich and others, 2003; Sturm and others, 2006; Iacozza and Barber, 2010; Petrich and others, 2012; Webster and others, 2015; Liston and others, 2018; Rösel and others, 2018; Moon and others, 2019). However, including the impacts of horizontal heat fluxes in net heat flux estimates would require measuring snow depths and ice thicknesses in a manner that retains their spatial relationships on a dense sampling grid. In fact, we are unaware of any measurement campaigns that have done so at sub-meter horizontal spacing and it may not be possible without disturbing the surface. Second, vertical-only heat flux simulation (Eqn. (3)) can be computed with a single line of Python (Rossum and Drake, 2010) code and trivial computational expense. Estimating three-dimensional heat fluxes (Eqns. (1) and (2)) is much more complicated and computationally expensive.

Finally, two prior studies have explicitly considered horizontal heat flux in Arctic sea ice. Sturm and others (2002b) simulated two-dimensional heat flux in a 40 m long transect of multi-year ice containing ice hummocks and refrozen melt ponds. They found that the spatially variable snow and ice cover resulted in a heat flux 40% greater than uniform snow and ice covers. However, they did not distinguish the impacts of snow spatial variability from ice spatial variability. Popović and others (2020) developed a mathematical model of the snow topography on level, first-year ice based upon the random placement of Gaussian mounds with a fixed aspect ratio. Based on this model, they derived functions relating the mean, variance, and semivariogram range to estimated heat flux for vertical-only and including horizontal cases. For three cases of level, first-year ice near Utqiaġvik, AK, they estimated that simulating vertical-only heat flux for a spatially variable snow cover increased net heat flux by 4–11% compared with a uniform snow cover. However, they estimated that including horizontal heat flux did not result in an increased net heat flux relative to vertical-only heat flux (<1% increase). Because of the smoothness of the Gaussian mounds, it is unclear that their model accurately represents the small-scale surface roughness of snow on sea ice.

We measured the snow surface topography on level, landfast, first-year ice in Elson Lagoon near Utqiaġvik, AK at horizontal resolutions of 3–15 cm. We use this topography to simulate conductive heat flux through snow and ice and estimate the impacts of snow spatial variability on the net heat flux by simulating vertical-only and including horizontal fluxes. For simulated 1-m-thick ice, we find that simulating vertical-only heat flux

https://doi.org/10.1017/jog.2023.105 Published online by Cambridge University Press

increases the net heat flux in the largest region we studied (Fig. 1c and Table 1) by 6% compared to a uniform snow cover with the same mean depth. Including horizontal fluxes increases the net flux by 10% (compared to uniform snow) for this region. However, if we had increased our horizontal measurement spacing to 1 m or greater, then including horizontal fluxes has almost no impact compared to the vertical-only simulations (Fig. 2)–supporting our hypothesis that sub-meter-scale spatial variability is important for horizontal heat flux. We discuss the implications of these results and make recommendations for future investigations of heat flux on Arctic sea ice in the Discussion.

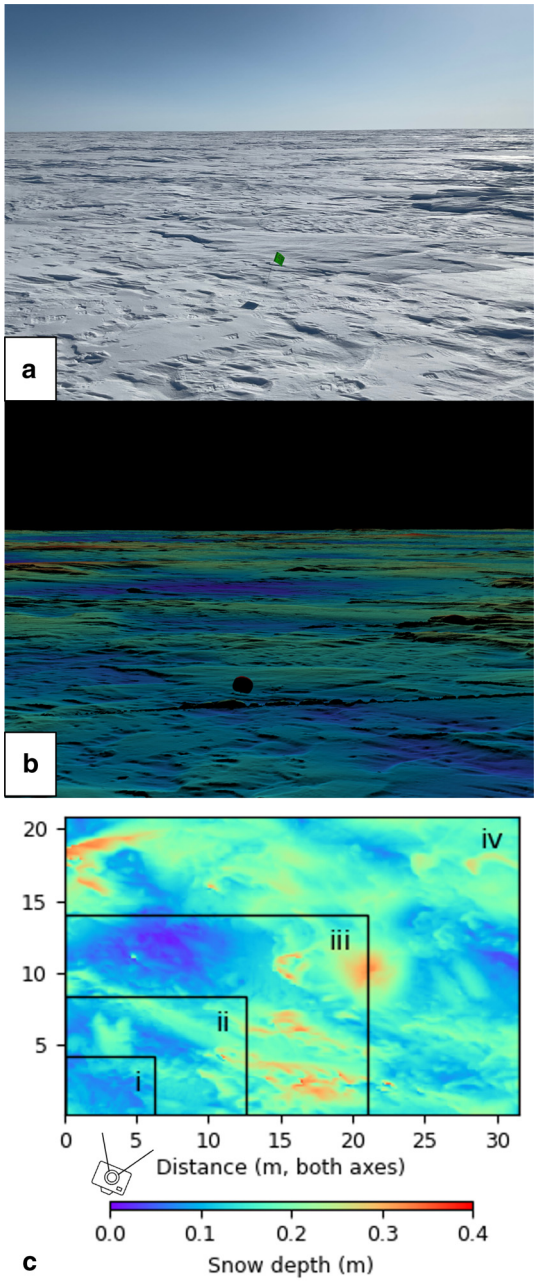

Figure 1. Study area in Elson Lagoon, AK on 17 April 2022: (a) photograph, (b) 3D rendering of TLS data (c) assumed snow depth map from TLS data. 3D rendering (b) is from approximately the same viewpoint as the photograph (a)–marked by camera glyph in (c). Camera lens distortion is not modeled. Lighting for 3D scene (b) is from the same elevation and azimuth as sun position in photograph (a) so that shadows generally correspond. The same colormap is used in (b) and (c). The nested regions used in the heat flux analysis are marked in (c). Photo credit for (a): Serina Wesen.

2. Materials and methods

2.1 Data collection and processing

We used a Riegl VZ1000 Terrestrial Laser Scanner (TLS) to measure the snow surface topography on an untrodden 200x50 m area of level, landfast, first-year ice in Elson Lagoon, AK (71.349°N, 156.526°W) on 17 April 2022 as part of the Snow ALbedo eVOlution (SALVO) project. TLS, an application of Light Detection and Ranging (LiDaR), is a standard technique for measuring snow topography (Deems and others, 2013) wherein a tripod-mounted laser scanner maps the surface using a line-of-sight laser emitter and detector. To measure the entire area, we collected TLS data from five scan positions arrayed around the outside of the 200 × 50 m area. We co-located the scan positions with one another within an uncertainty of 3 mm using Riegl 10 cm reflectors mounted on posts frozen into the ice and a plane-matching algorithm in RiSCAN (Riegl's software for TLS acquisition and processing). The ranging precision of the VZ1000 is 5 mm and the beam divergence is 0.3 mrad.

We selected four nested regions in the center of the untrodden measurement area near the central scan position (where our measurement resolution was highest) to simulate heat flux (Fig. 1c and Table 1). For each region, we converted the TLS pointcloud data to gridded data by first constructing a triangulated surface from the pointcloud (Kazhdan and others, 2006) and then sampling this surface at the desired resolution. For the higher resolution regions, the sizes of the regions were limited by our desire to keep the percentage of grid cells without TLS measurement points in them at less than 5% (admittedly an arbitrary cutoff). The size of the largest region was motivated by a desire to exceed the typical structural length scale of 20 m (the distance beyond which the snow depths become uncorrelated; Sturm and others, 2002a; Itkin and others, 2023). Simulating 3D heat flux on domains larger than our largest region was computationally infeasible with our available resources.

2.2 Heat flux simulation

Since our interest is the impact of the snow variability, we will assume that the ice is uniformly 1 m thick with level ocean-ice and ice-snow interfaces (Popović and others, 2020, makes the same assumptions, so these choices facilitate comparing our results). Because ice in Elson Lagoon is first year ice that is protected from substantial ice dynamics, the assumptions of level interfaces is reasonable (e.g., Webster and others, 2014, note also the generally level character of the ice extending to the horizon in Figure 1). We set the same vertical position of the snow-ice interface for all of the regions (as is sensible since they are overlapping) such that all snow depths are greater than 1 cm–consistent with our observation that all ice was snow covered. With these assumptions, the coefficients of variation of snow depth (Table 1) in the larger regions fall within the range typically observed for snow on level, first-year ice.

For each region, we convert the snow and ice volume into a three-dimensional tetrahedral mesh using Gmsh (Geuzaine and Remacle, 2009). We assume constant ocean-ice and snow-air interface temperatures (Dirichlet boundary conditions) and that there is no horizontal heat flux at the lateral borders of the domains (Neumann boundary conditions). We set the snow thermal conductivity at 0.14 W m^{-1} K^{-1} and ice thermal conductivity at 2.0 W m^{-1} K^{-1} (same values used by Popović and others, 2020). For each region, we numerically solve Eqns. (1) and 2 via the Finite Element Method using second-order Lagrange elements (using FEniCS: Kirby, 2004; Kirby and Logg, 2006; Kirby, 2012; Logg and Wells, 2010; Logg and others, 2012a, 2012b, 2012c; Ølgaard and Wells, 2010; Alnaes and others, 2014;

https://doi.org/10.1017/jog.2023.105 Published online by Cambridge University Press

Table 1. Summary statistics and simulated heat fluxes for each region in Figure 1c.

Region	Resolution (cm)	Size (m)	Point density (# m^{-2})	Mean snow depth (cm)	Standard deviation snow depth (cm)	Coefficient of variation	Heat flux incl. horizontal (W m^{-2})	Heat flux vertical-only (W m^{-2})	Heat flux uniform snow (W m^{-2})
i	3	6.3 × 4.2	5.6×10^3	10	2	0.21	16.42	16.30	16.05
ii	6	12.6 × 8.4	3.5×10^3	13	4	0.29	14.51	14.26	13.77
iii	10	21 × 14	2.0×10^3	15	6	0.41	14.41	14.00	12.94
iv	15	31.5 × 21	1.2×10^3	15	5	0.34	13.69	13.21	12.46

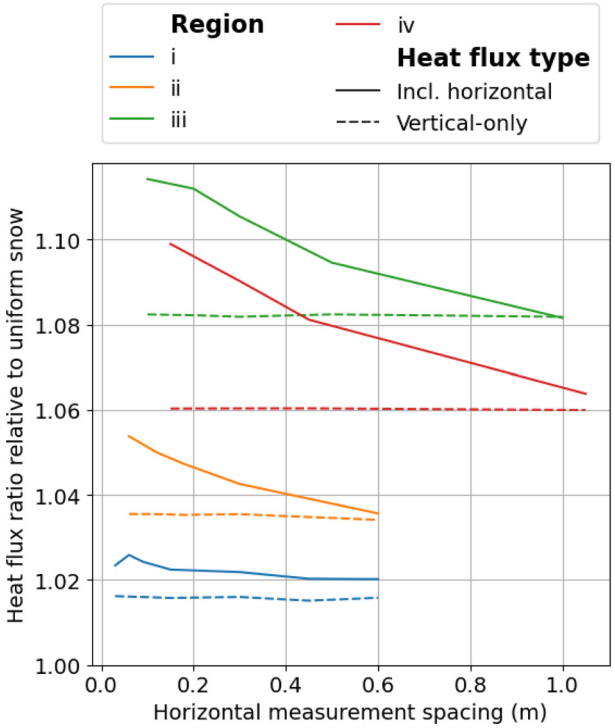

Figure 2. Comparison of how increasing the horizontal measurement spacing (i.e., degrading the resolution) impacts simulated heat flux ratios relative to a uniform snow cover for simulations of vertical-only heat flux and including horizontal fluxes on each region in Figure 1c. Increasing measurement spacing does not impact the vertical-only heat flux ratios (dashed lines), but does reduce the horizontal heat flux ratios (solid).

Alnæs and others, 2015; Scroggs and others, 2022) assuming a 20 K temperature difference between the ocean-ice and snow-air interfaces. Note that this is a simplified version of Eqns. (1) and (2) where $\kappa(x, y, z)$ is either κ_s or κ_i in the snow and ice respectively. We numerically integrated the vertical heat flux at the ocean-ice interface to estimate the net mean heat flux. For each region, we also estimated the vertical-only heat flux (for the assumed spatially variable snow cover) and the heat flux assuming uniform snow thickness with Eqn. (3). Finally, to investigate the impacts of the measurement resolution on the results, we downsampled the gridded snow topographies by factors of 2–20 and computed the heat fluxes.

3. Results

Including horizontal heat flux simulated more total heat flux than that simulated with vertical-only heat flux and the heat flux assuming uniform snow depth (Table 1 and Fig. 2). Increasing the horizontal measurement spacing (i.e., degrading the resolution) does not affect the ratio between the simulated vertical-only heat fluxes and that simulated with a uniform snow cover (the dashed lines are roughly constant in Fig. 2). However, increasing the measurement spacing reduces the impact of including horizontal fluxes in the simulation (the solid lines decrease to the right in Fig. 2). When the horizontal measurement spacing is 1 m or greater, we do not find that including horizontal heat fluxes resulted in a net heat flux greater than the vertical-only simulations. We also examined the sensitivity of our results to ice thickness by simulating region iii with an ice thickness of 2 m (not shown). The overall magnitude of the heat flux decreased, as expected for thicker ice, but the relative effect of including horizontal heat flux was similar. Additionally, we explored the sensitivity of our results to increasing the snow thermal conductivity to 0.3 W m^{-1} K−1 (Supplemental Material: Table S1 and Fig. S1). This does not change the relative effect of including horizontal heat flux, but does decrease the impact of snow depth variability on heat flux. For example, for region iv at 15 cm resolution, including horizontal heat flux results in 6% greater heat flux than a uniform snow cover, whereas vertical-only heat flux is 3% greater than a uniform snow cover. For comparison, with snow thermal conductivity of 0.14 W m^{-1} K−1, for region iv at the 15 cm horizontal resolution, including horizontal heat flux results in 10% greater heat flux than a uniform snow cover, whereas vertical-only heat flux is only 6% greater than a uniform snow cover.

4. Discussion and conclusion

The simulation results generally confirm the intuition from the thought experiment in the Motivation: sub-meter-scale snow depth variability increases the net heat flux when our simulations include horizontal fluxes. Furthermore, in this case, the additional net simulated heat fluxes when including horizontal fluxes relative to vertical-only simulations were a similar magnitude, albeit smaller, to the impacts of simulating vertical-only fluxes in a spatially variable snow cover compared to a uniform snow cover. This contradicts the results of Popović and others (2020), although we made the same assumptions about ice thickness and snow and ice thermal conductivities. Popović and others (2020) reported that simulating horizontal fluxes had no impact on the net heat flux beyond vertical-only simulation. We suspect that their model, which represents snow dunes as smooth Gaussian mounds, is not accurately representing sub-meter-scale snow variability. When we downsample our data to horizontal measurement spacings of 1 m or greater, including horizontal heat fluxes no longer simulates additional net heat flux compared to vertical-only simulations (i.e., the same result as Popović and others, 2020). The modeling approaches are also different, Popović and others (2020) derived analytical mathematical relationships between summary statistics (mean, variance, and semivariogram range) and heat flux whereas we conducted finite element simulations with a specific, measured snow topography.

The impacts of degrading the horizontal resolution were qualitatively similar for all four nested regions: degrading the resolution reduced the heat flux simulated when including horizontal fluxes but did not impact the vertical-only simulations. The smaller regions (i and ii) were included to assess whether any novel behavior occurred at extremely high (<10 cm) sampling resolution (e.g., a dramatic increase in the heat flux simulated when including horizontal fluxes), and because technical

https://doi.org/10.1017/jog.2023.105 Published online by Cambridge University Press

limitations prevented us from measuring such high resolution topography on larger domains. However, using such small domains introduces quantitative differences in simulated heat fluxes between the regions that are due to the domain size. Most importantly, the variance of snow depth in small regions (e.g., i and ii) tends to be less than that in larger regions (e.g., iii and iv), because snow depth is spatially auto-correlated at distances less than the semivariogram range (typically around 20 m). When snow depth variance is lower (small regions), the impacts of depth variability are smaller (i.e., uniformity is a better approximation). Consider the limiting behavior. If our entire domain were a column of snow and ice with infinitessimal horizontal extent, then all three types of simulated heat flux would be identical. For regions i and ii, sampling resolutions of less than 15 cm (the resolution of region iv) caused insignificant differences in the simulated heat flux (<0.05 W m^{-2}). Thus we conclude that the sampling resolution of the larger regions (iii and iv) was sufficient to observe these effects. Since the larger regions are less affected by autocorrelation, we expect them to be more representative of large-scale effects although further work with more computational resources could help extend this analysis to larger domains.

Quantitatively assessing the representativeness of the sub-meter-scale snow roughness on this particular region of level, first-year Arctic sea ice is beyond the scope of this study (and likely requires more data collection of high resolution surface topography). However, the assumed mean, standard deviation, and coefficient of variation of snow depths for our two larger regions (iii and iv) are within the range of typical values on level, first-year Arctic sea ice (Iacozza and Barber, 1999; Sturm and others, 2002a; Petrich and others, 2012; Webster and others, 2015; Moon and others, 2019, the mean and standard deviation are at approximately the 25 percentile, the coefficient of variation is near the median).

Assessing the importance of horizontal heat flux enhancement on large spatial or temporal scales is challenging because there are almost no measurements of sub-meter-scale snow thickness variability. This includes this study, we could only measure snow topography and infer depth based on level-ice assumptions. Collecting TLS scans prior to the first snowfall (as is sometimes done in terrestrial environments: e.g., Hartzell and others, 2015) could address this data gap, although this is logistically challenging on sea ice. Another approach would be targeted studies to see if the fractal-scaling behavior observed in super-meter-scale snow depth (Deems and others, 2006; Trujillo and others, 2007, 2009; Moon and others, 2019) extends to sub-meter-scales on Arctic sea ice. If so, information about sub-meter-scale variability could be inferred from super-meter-scale measurements. Regarding models of the snow and ice cover, our results suggest that if they seek to simulate the impact of horizontal heat fluxes, they should represent sub-meter-scale snow depth variability. How exactly, to simulate or parameterize this variability will require more measurements and process studies of sub-meter-scale variability. Finally, although we consider a single field site and assumed uniform ocean-ice and ice-snow interfaces, the order of magnitude of the heat flux enhancements we simulate may be of use to other researchers. For our largest region (iv), the simulated heat flux is 10% greater including horizontal heat flux than that for uniform snow with the same mean snow thickness. Whereas, simulating vertical-only fluxes increased the net simulated heat flux by 6%.

Supplementary material. The supplementary material for this article can be found at https://doi.org/10.1017/jog.2023.105

Data. TLS data used in this work are available at Clemens-Sewall (2023b). A Python package for processing and manipulating TLS data is available at Clemens-Sewall (2023a) and described in Clemens-Sewall and others (2024).

Acknowledgements. Observations of landfast sea ice in Utqiaġvik, AK were made on Iñupiat lands and permitted by the North Slope Borough and the Ukpeaġvik Inupiat Corporation. The field campaign was supported by UIC Science. UIC Science obtains permission from the Barrow Whaling Captains Association for accessing landfast ice during the whaling season.

DCS was supported by NSF OPP-1724540 and NSF OPP-2138788. CP, and DP were supported by NSF OPP-1724540 and NSF OPP-2138785. MAW was supported primarily by the U.S. Department of Energy's Atmospheric System Research, an Office of Science Biological and Environmental Research program, under DE-SC0019107. Logistical support was provided by the Department of Energy's Atmospheric System Research program (DE-SC0019107) and the Atmospheric Radiation Measurement Program as part of the 2022 SALVO field campaign. Data utilized in this study were collected as part of the Sea Ice Dynamics Experiment (SIDEx), funded by the Office of Naval Research under award N00014-19-1-2603. We gratefully acknowledge the help and cooperation of the large team of scientific collaborators, logistics providers, and operational support centers associated with the SIDEx project effort.

We thank Matthew Sturm, Jen Delamere, Ema Mayo, Anika Pinzner, Phillip Wilson, David Shean, and Serina Wesen for their capable assistance in the field. Special thanks to Matthew Sturm whose work piqued our interest in the topic and whose encouragement contributed to its completion.

References

Abraham C, Steiner N, Monahan A and Michel C (2015) Effects of subgrid-scale snow thickness variability on radiative transfer in sea ice. *Journal of Geophysical Research: Oceans* **120**(8), 5597–5614. doi:10.1002/2015JC010741

Alnaes MS, Rognes ME, Logg A, Ølgaard KB and Wells GN (2014) Unified form language: a domain-specific language for weak formulations of partial differential equations. *ACM Transactions on Mathematical Software* **40**, 1–37. doi: 10.1145/2566630

Alnæs M and 9 others (2015) The FEniCS project version 1.5. *Archive of Numerical Software* **3**(100), 9–23.

Calonne N, Geindreau C and Flin F (2014) Macroscopic modeling for heat and water vapor transfer in dry snow by homogenization. *The Journal of Physical Chemistry B* **118**(47), 13393–13403. doi: 10.1021/jp5052535

Clemens-Sewall D (2023a) davidclemenssewall/pydar: v1.0.0.

Clemens-Sewall D (2023b) High-Resolution Topography of Landfast ice in Elson Lagoon, AK from Terrestrial Laser Scanning from the Snow ALbedo eVOlution campaign April 2022.

Clemens-Sewall D and 12 others (2024) High-resolution repeat topography of drifting ice floes in the Arctic Ocean from terrestrial laser scanning. *Scientific Data* **11**(1), 70. doi: 10.1038/s41597-023-02882-w

Colbeck SC (1997) A Review of Sintering in Seasonal Snow. CRREL Report 97-10. US Army Corps of Engineers Cold Regions Research & Engineering Laboratory, Hanover, NH.

Deems JS, Fassnacht SR and Elder KJ (2006) Fractal distribution of snow depth from lidar data. *Journal of Hydrometeorology* **7**(2), 285–297. doi: 10.1175/JHM487.1

Deems JS, Painter TH and Finnegan DC (2013) Lidar measurement of snow depth: a review. *Journal of Glaciology* **59**(215), 467–479. doi: 10.3189/2013JoG12J154

Fourier JBJ (1822) *Théorie analytique de la chaleur*. Paris: F. Didot.

Geuzaine C and Remacle JF (2009) Gmsh: A 3-D finite element mesh generator with built-in pre- and post-processing facilities. *International Journal for Numerical Methods in Engineering* **79**(11), 1309–1331. doi: 10.1002/nme.2579

Hanson AM (1965) Studies of the mass budget of arctic pack-ice floes. *Journal of Glaciology* **5**(41), 701–709. doi: 10.3189/S0022143000018694

Hanson AM (1980) The snow cover of sea ice during the arctic ice dynamics joint experiment, 1975 to 1976. *Arctic and Alpine Research* **12**(2), 215–226. doi: 10.1080/00040851.1980.12004180

Hartzell PJ, Gadomski PJ, Glennie CL, Finnegan DC and Deems JS (2015) Rigorous error propagation for terrestrial laser scanning with application to snow volume uncertainty. *Journal of Glaciology* **61**(230), 1147–1158. doi: 10.3189/2015JoG15J031

Iacozza J and Barber DG (1999) An examination of the distribution of snow on sea-ice. *Atmosphere-Ocean* **37**(1), 21–51. doi: 10.1080/07055900.1999.9649620

Iacozza J and Barber DG (2010) An examination of snow redistribution over smooth land-fast sea ice. *Hydrological Processes* **24**(7), 850–865. doi: 10.1002/hyp.7526

Isaaks E and Srivastava R (1989) *An introduction to applied geostatistics*. New York: Oxford University Press, 561 p.

Itkin P and 12 others (2023) Sea ice and snow characteristics from year-long transects at the MOSAiC Central Observatory. *Elementa: Science of the Anthropocene* **11**(1), 00048. doi: 10.1525/elementa.2022.00048

Kazhdan M, Bolitho M and Hoppe H (2006) Poisson surface reconstruction. In *Proceedings of the fourth Eurographics symposium on Geometry processing*, Vol. 7, Goslar, Germany.

Kirby RC (2004) Algorithm 839: FIAT, a new paradigm for computing finite element basis functions. *ACM Transactions on Mathematical Software* **30**, 502–516. doi: 10.1145/1039813.1039820

Kirby RC (2012) FIAT: Numerical Construction of Finite Element Basis Functions. In Anders Logg, Kent-Andre Mardal, Garth Wells (eds), *Automated Solution of Differential Equations by the Finite Element Method*, volume 84 of *Lecture Notes in Computational Science and Engineering*. Berlin, Germany: Springer.

Kirby RC and Logg A (2006) A compiler for variational forms. *ACM Transactions on Mathematical Software* **32**, 417–444. doi: 10.1145/1163641.1163644

Laplace PS (1822) *A Treatise of Celestial Mechanics*. Richard Milliken and for Longman, Hurst, Rees, Orme and Browne, London. Google-Books-ID: 4xUGh3q36D4C.

Liston GE and 6 others (2018) A distributed snow-evolution model for sea-ice applications (SnowModel). *Journal of Geophysical Research: Oceans* **123**(5), 3786–3810. doi: 10.1002/2017JC013706

Logg A and Wells GN (2010) DOLFIN: Automated Finite Element Computing. *ACM Transactions on Mathematical Software* **37**, 1–28. doi: 10.1145/1731022.1731030

Logg A, Wells GN and Hake J. (2012a) DOLFIN: a C++/Python Finite Element Library. In Anders Logg, Kent-Andre Mardal, Garth Wells (eds), *Automated Solution of Differential Equations by the Finite Element Method*, volume **84** of *Lecture Notes in Computational Science and Engineering*. Berlin, Germany: Springer, section: 10.

Logg A, Wea GN and Mardal K-A (2012b) *Automated Solution of Differential Equations by the Finite Element Method*. Berlin, Germany: Springer.

Logg A, Rlgaard ME, Ølgaard KB and Wells GN (2012c) FFC: the FEniCS Form Compiler. In Anders Logg, Kent-Andre Mardal, Garth Wells (eds), *Automated Solution of Differential Equations by the Finite Element Method*, volume **84** of *Lecture Notes in Computational Science and Engineering*. Berlin, Germany: Springer, section: 11.

Mallett RDC and 10 others (2022) Sub-kilometre scale distribution of snow depth on Arctic sea ice from Soviet drifting stations. *Journal of Glaciology* **68**(271), 1014–1026. doi: 10.1017/jog.2022.18

Moon W and 11 others (2019) Physical length scales of wind-blown snow redistribution and accumulation on relatively smooth Arctic first-year sea ice. *Environmental Research Letters* **14**(10), 104003. doi: 10.1088/1748-9326/ab3b8d

Niedrauer TM and Martin S (1979) An experimental study of brine drainage and convection in Young Sea ice. *Journal of Geophysical Research: Oceans* **84**(C3), 1176–1186. doi: 10.1029/JC084iC03p01176

Notz D and SIMIP Community (2020) Arctic sea ice in CMIP6. *Geophysical Research Letters* **47**(10), e2019GL086749. doi: 10.1029/2019GL086749

Ølgaard KB and Wells GN (2010) Optimisations for quadrature representations of finite element tensors through automated code generation. *ACM Transactions on Mathematical Software* **37**, 1–23. doi: 10.1145/1644001.1644009

Perovich DK and 5 others (2003) Thin and thinner: sea ice mass balance measurements during SHEBA. *Journal of Geophysical Research: Oceans* **108**(C3), 8050. doi: 10.1029/2001JC001079

Petrich C and 6 others (2012) Snow dunes: a controlling factor of melt pond distribution on Arctic sea ice. *Journal of Geophysical Research: Oceans* **117**, C09029. doi: 10.1029/2012JC008192

Popović P, Finkel J, Silber MC and Abbot DS (2020) Snow topography on undeformed Arctic sea ice captured by an idealized 'snow dune' model. *Journal of Geophysical Research: Oceans* **125**(9), e2019JC016034. doi: 10.1029/2019JC016034

Radionov VF, Bryazgin NN and Alexandrov EI (1997) The Snow Cover of the Arctic Basin. Technical report, Washington Univ Seattle applied physics lab, section: Technical Reports.

Rösel A and 7 others (2018) Thin sea ice, thick snow, and widespread negative freeboard observed during N-ICE2015 North of Svalbard. *Journal of Geophysical Research: Oceans* **123**(2), 1156–1176. doi: 10.1002/2017JC012865

Rossum Gv and Drake FL (2010) *The Python language reference*. Number Pt. 2 in Python documentation manual / van Rossum G and Drake FL [ed.], Python Software Foundation, Hampton, NH, release 3.0.1 [repr.] edition.

Screen JA and Simmonds I (2010) The central role of diminishing sea ice in recent Arctic temperature amplification. *Nature* **464**(7293), 1334–1337. doi: 10.1038/nature09051

Scroggs MW, Dokken JS, Richardson CN and Wells GN (2022) Construction of arbitrary order finite element degree-of-freedom maps on polygonal and polyhedral cell meshes. *ACM Transactions on Mathematical Software* **48**(2), 1–23. doi: 10.1145/3524456

Semtner AJ (1976) A model for the thermodynamic growth of sea ice in numerical investigations of climate. *Journal of Physical Oceanography* **6** (3), 379–389. doi: 10.1175/1520-0485(1976)006<0379:AMFTTG>2.0.CO;2

Sturm M and Johnson JB (1991) Natural convection in the subarctic snow cover. *Journal of Geophysical Research: Solid Earth* **96**(B7), 11657–11671. doi: 10.1029/91JB00895

Sturm M, Holmgren J and Perovich DK (2002a) Winter snow cover on the sea ice of the Arctic Ocean at the Surface Heat Budget of the Arctic Ocean (SHEBA): Temporal evolution and spatial variability. *Journal of Geophysical Research: Oceans* **107**(C10), 8047. doi: 10.1029/2000JC000400

Sturm M, Perovich DK and Holmgren J (2002b) Thermal conductivity and heat transfer through the snow on the ice of the Beaufort Sea. *Journal of Geophysical Research: Oceans* **107**(C10), 8043. doi: 10.1029/2000JC000409

Sturm M and 8 others (2006) Snow depth and ice thickness measurements from the Beaufort and Chukchi seas collected during the AMSR-Ice03 campaign. *IEEE Transactions on Geoscience and Remote Sensing* **44**(11), 3009–3020. doi: 10.1109/TGRS.2006.878236

Thielke L and 5 others (2021) Helicopter-borne thermal infrared sea ice surface temperature images during the MOSAiC expedition, NetCDF format.

Trujillo E, Ramírez JA and Elder KJ (2007) Topographic, meteorologic, and canopy controls on the scaling characteristics of the spatial distribution of snow depth fields. *Water Resources Research* **43**, W07409. doi: 10.1029/2006WR005317

Trujillo E, Ramírez JA and Elder KJ (2009) Scaling properties and spatial organization of snow depth fields in sub-alpine forest and alpine tundra. *Hydrological Processes* **23**(11), 1575–1590. doi: 10.1002/hyp.7270

Urrego-Blanco JR, Urban NM, Hunke EC, Turner AK and Jeffery N (2016) Uncertainty quantification and global sensitivity analysis of the Los Alamos sea ice model. *Journal of Geophysical Research: Oceans* **121**(4), 2709–2732. doi: 10.1002/2015JC011558

Webster MA and 6 others (2014) Interdecadal changes in snow depth on Arctic sea ice. *Journal of Geophysical Research: Oceans* **119**(8), 5395–5406. doi: 10.1002/2014JC009985

Webster MA and 5 others (2015) Seasonal evolution of melt ponds on Arctic sea ice. *Journal of Geophysical Research: Oceans* **120**(9), 5968–5982. doi: 10.1002/2015JC011030

https://doi.org/10.1017/jog.2023.105 Published online by Cambridge University Press